

1 **Title**

2 **Commensal bacteria act as a broad genetic buffer in *Drosophila* during chronic
3 under-nutrition**

4

5 **Authors**

6 Dali Ma¹, Maroun Bou-Sleiman^{2,3}, Pauline Joncour¹, Claire-Emmanuelle Indelicato¹,
7 Michael Frochaux², Virginie Braman², Maria Litovchenko², Gilles Storelli^{1,4}, Bart
8 Deplancke ^{2*}, François Leulier^{1*}

9

10 **Affiliations**

11 1. Institut de Génomique Fonctionnelle de Lyon (IGFL), Université de Lyon, Ecole
12 Normale Supérieure de Lyon, Centre National de la Recherche Scientifique, Université
13 Claude Bernard Lyon 1, Unité Mixte de Recherche 5242, 69364 Lyon, Cedex 07, France

14

15 2. Laboratory of Systems Biology and Genetics, Institute of Bioengineering and Swiss
16 Institute of Bioinformatics, School of Life Sciences Ecole Polytechnique Federale de
17 Lausanne (EPFL) CH-1015, Lausanne, Switzerland

18

19 3. Present address: Laboratory of Integrative Systems Physiology, Interschool Institute of
20 Bioengineering, School of Life Sciences, Ecole Polytechnique Federale de Lausanne
21 (EPFL) CH-1015, Lausanne, Switzerland

22

23 4. Present address: Department of Human Genetics, University of Utah School of
24 Medicine, Salt Lake City, UT 84112, USA

25

26 * co-corresponding authors

27 bart.deplancke@epfl.ch and francois.leulier@ens-lyon.fr

28

29

30 **Summary**

31 Eukaryotic genomes encode several well-studied buffering mechanisms that robustly
32 maintain invariant phenotypic outcome despite fluctuating environmental conditions.
33 Here we show that the gut microbiota, represented by a single *Drosophila* facultative
34 symbiont, *Lactobacillus plantarum* (Lp^{WJL}), acts also as a broad genetic buffer that masks
35 the contribution of the cryptic genetic variations in the host under nutritional stress.
36 During chronic under-nutrition, Lp^{WJL} consistently reduces variation in different host
37 phenotypic traits and ensures robust organ patterning; Lp^{WJL} also decreases genotype-
38 dependent expression variation, particularly for development-associated genes. We
39 further demonstrate that Lp^{WJL} buffers via reactive oxygen species (ROS) signaling whose
40 inhibition severely impairs microbiota-mediated phenotypic robustness. We thus
41 identified an unexpected contribution of facultative symbionts to *Drosophila* fitness by
42 assuring developmental robustness and phenotypic homogeneity in times of nutritional
43 stress.

44

45

46 **Key Words**

47 microbiota; cryptic genetic variations; phenotypic robustness; ROS; robustness; buffer

48

49

50

51

52

53

54

55

56

57

58

59

60

61

62

63

64 **Results and Discussions**

65 *Mono-association with *Lp*^{WJL} reduces growth/size variation of *Drosophila* larvae during*

66 *chronic under-nutrition in the DGRP lines*

67 Despite environmental stress, organisms possess intrinsic genetic buffering mechanisms
68 to maintain phenotypic constancy by repressing the expression of cryptic genetic variants,
69 thus preserving genetic diversity. Compromising these buffering mechanisms unlocks
70 new substrates for natural selection[1-3]. However, natural selection can also operate on
71 the hologenome, as symbiosis is recognized as a major driving force of evolution [4, 5].
72 Facultative nutritional mutualism forged by the host and its resident gut microbiota
73 permits the holobiont to adapt to changing nutritional environments during the host's life
74 time[6]. Consequently, the evolutionary implications of such association deserve more
75 scrutiny. Horizontally acquired gut bacteria in *Drosophila* are a perfect example of
76 nutritional mutualists[7]. Previously, we showed that a single commensal strain, *Lp*^{WJL}
77 can significantly accelerate growth in ex-germ free (GF) larvae during chronic under-
78 nutrition[8, 9]. To study the host's genetic contribution to *Lp*^{WJL}-mediated growth in the
79 same context, we first measured the body lengths of both the GF and *Lp*^{WJL} mono-
80 associated larvae from 53 DGRP lines 7 days after post-embryonic development (Fig.1a-
81 c; Table S1), and conducted genome-wide association studies (GWAS) based on the
82 ranking of growth gain by comparing GF and *Lp*^{WJL}-associated animals (Fig.1a; TableS1,
83 column "ratio"). The GWAS yielded nine candidate variants (Table S2, Fig.S1a and
84 S1b), and through RNA interference (RNAi), we assessed the contribution of each
85 variant-associated gene to host growth with or without *Lp*^{WJL}. Surprisingly, we failed to
86 capture any obvious "loss or gain of function" of the growth benefit conferred by *Lp*^{WJL}.
87 Instead, we observed that the individual RNAi-mediated knock-down of gene expression
88 led to large phenotypic variation in GF larvae, but such variation was reduced in *Lp*^{WJL},
89 resulting in growth gain in all tested genetic backgrounds (Fig.S1c and S1d). In parallel,
90 we computed the respective heritability estimates (H) for the GF and *Lp*^{WJL} -associated
91 DGRP populations as 37% vs. 10% (Fig.1b and 1c). The coefficient of variation (CV) of
92 the pooled GF population was also greater, despite their overall smaller standard
93 deviation and average size (Fig.1d). These three observations strongly indicate that
94 genetic variants induce more pronounced size variation in GF animals, and the gut
95 bacteria unexpectedly restrict growth variation despite host genetic differences. Next, we
96 plotted the individual average GF larval length value against that of its *Lp*^{WJL} -associated
97 siblings from both the DGRP and the RNAi studies and derived the linear regression

98 coefficients. If genetic background predominantly impacts growth, then this coefficient
99 should be close to 1, yet we found that both are close to zero (0.145 and 0.06
100 respectively; Fig.1e and Fig.S1e). We thus conclude that Lp^{WJL} presence effectively
101 masks the contribution of genetic variation in the DGRP lines and steers the animals
102 toward attaining a similar size independent of genotype.

103

104 *Mono-association with Lp^{WJL} decreases expression variation of developmentally-related
105 genes during growth*

106 Since Lp^{WJL} reduces growth variation in the host phenotypically, and phenotypic variation
107 is often the manifestation of transcriptomic variation due to genetic differences[10], we
108 explored if Lp^{WJL} also decreases gene expression variation during larval development. We
109 conducted BRB-seq[11] on 36 mono-associated and 36 GF individual larvae from 3
110 DGRP lines and specifically compared transcriptional variation in individual Lp^{WJL}
111 mono-associated larvae to that of age-matched GF samples (Fig.S2a). First, we observed
112 that the transcriptomes tend to cluster by genotype and Lp^{WJL} status after batch effect
113 correction (Fig.S2b and S2c, Table S3). Second, the overall transcriptomic changes and
114 the GO-terms associated with Lp^{WJL} presence corroborate our previous findings, as
115 similar sets of digestive enzymes and immune response genes were up-regulated (Fig.S2d
116 and S2e)[12]. Interestingly, genotype was a stronger clustering driver for GF samples
117 than Lp^{WJL} mono-associated ones when samples were separated based on bacterial
118 presence (Fig 1f vs. 1h, and 1g vs. 1i). These observations suggest that Lp^{WJL} can mask
119 host genetic differences also at the transcriptomic level. Next, we compared the standard
120 deviation (SD) of each expressed gene in both conditions, and found that even though
121 mono-association can either elevate or reduce expression variation in different gene sets
122 (Fig.S2f and S2g), there is a tendency toward an overall increase in expression variation
123 in GF transcriptomes (Fig.S2f, red line). This trend was also more apparent in genes that
124 were non-differentially expressed between the GF and mono-associated conditions (Fig.S1h, middle panel, grey lines). Finally, we found that genes whose expression
125 variation most-decreased by Lp^{WJL} are enriched in developmental processes such as
126 “body morphogenesis” and “cuticle development” (Fig.1j). These data reveal that Lp^{WJL}
127 mono-association dampens genotype-dependent expression variation, especially of genes
128 linked to developmental processes, which in turn may account for the ability of Lp^{WJL} to
129 reduce larval size variation.

131

132 *Lp^{WJL}* broadly buffers variation in different physical fitness traits in genetically diverse
133 populations

134 Based on these findings, we propose that *Lp^{WJL}* effectively reduces both phenotypic and
135 transcriptional fluctuations during chronic under-nutrition. *Lp^{WJL}* thus confers a biological
136 function that resembles various canonical buffering mechanisms that robustly maintain
137 phenotypic homogeneity by masking the effects of cryptic genetic variation[2, 13, 14],
138 despite the presence of a persistent nutritional stress signal. Since our studies insofar were
139 conducted only in homozygous inbred DGRP lines, we sought to test if the observed
140 buffering also operates in a population of heterozygous and genetically diverse
141 individuals. Therefore, based on their GF growth profile, we selected two DGRP strains
142 from each end of the phenotypic extremes (Fig.1b and 1c, patterned pink and blue bars),
143 established seven different inter-strains crosses, and compared the growth variation in the
144 GF and mono-associated F₂ progenies (Fig.S3a, Methods). In these experiments, we
145 supplemented the GF larvae with 33% more yeast (8g.L⁻¹ vs 6g.L⁻¹) to address two
146 possible caveats: first, we wished to exclude that *Lp^{WJL}* might simply act as an additional
147 food source, even though our previous findings indicate that this is not the case[7].
148 However, if increasing the dietary yeast content reduces the variability in GF growth to
149 the same extent as the gut bacteria, then the buffering effect may be generally attributed
150 to mere superior food quality. Second, greater yeast content accelerates GF growth;
151 consequently, the size and stage differences between the GF and mono-associated larvae
152 are minimized, thus allowing us to compare variation in size-matched GF and mono-
153 associated larvae *en masse*, while excluding the bias that bigger and older mono-
154 associated larvae might vary less as they tend to be more mature.

155

156 Our hypothesis predicts that the GF F₂ population should show higher variance in body
157 length than their *Lp^{WJL}* mono-associated siblings. Indeed, in the F₂ larvae, the CV and SD
158 values tend to separate into two distinct groups, as driven by *Lp^{WJL}* presence (Fig.2a,
159 Fig.S3b). Overall, the F₂ *Lp^{WJL}* mono-associated larvae were slightly longer, but their GF
160 siblings varied more in length, regardless of yeast content or larval age (Fig.S3c). In the
161 size-matched pools (Fig.2a, purple bracket), GF size still fluctuated more than that of the
162 *Lp^{WJL}* mono-associated siblings (Fig.2b), despite the fact that they were fed with a richer
163 diet. Based on these observations, we first confirm that augmenting yeast content fails to
164 recapitulate the same buffering effect mediated by living commensals. More importantly,
165 we conclude that phenotypic buffering by the gut microbe *Lp^{WJL}* indeed operates in a

166 genetically diverse host population facing a nutritional challenge, hence qualifying the
167 gut microbiota as a previously unappreciated buffering agent of cryptic genetic variation.

168

169 During chronic under-nutrition, Lp^{WJL} sustains growth rate as effectively as an entire gut
170 microbiota[8]. We thus wondered if a natural and more complex gut microbiota can also
171 buffer growth variation like Lp^{WJL} . To address this question, we rendered a population of
172 wild flies collected in a nearby garden germ-free, and re-associated them with their own
173 fecal microbial community[15]. In three out of four experimental repeats, growth
174 variation is significantly reduced in the larval population fed on food inoculated with
175 fecal microbiota (Fig.S3d and data not shown), and the cumulative CV and variances
176 derived from each food cap were significantly higher in the GF population (Fig.S3e and
177 S3f). This strongly suggests that the gut-associated microbial community of wild flies
178 indeed decreases growth variation of a natural *Drosophila* population. However, since the
179 wild-derived microbiota did not consistently buffer larval growth, probably due to the
180 difficulty to precisely control the quantity and composition of the inoculated fecal
181 microbiota, we returned to the mono-association model for subsequent studies.

182

183 If the observed growth variation in GF larvae indeed reflects the “unleashing” of the
184 host’s genetic potential due to the loss of a buffering mechanism provided by gut
185 microbes[2], then we hypothesized that other physical fitness traits in a fertile surviving
186 GF population should in principle also exhibit greater phenotypic variation. We therefore
187 examined the variances in pupariation timing and adult emergence in the F_2 progeny of
188 the inter-DGRP strain crosses (Fig.S3a). First, individual GF larvae pupariated and
189 eclosed later, but the variances in the pooled data were greater than that of mono-
190 associated counterparts (Fig.2c and 2d); from each vial containing an equal number of
191 larvae, the variances of pupariation and eclosion were also greater in the GF samples
192 (Fig.2e and 2f). Therefore, both inter-individual and among-population variances in
193 developmental timing and adult emergence are reduced. Lastly, GF adults were slightly
194 shorter (Fig.2g); the sizes of representative organs, expressed as area of the eye and the
195 wing, were also smaller, yet the variances in these traits were greater (Fig.2h, Fig.S3g).
196 Furthermore, the wing/body-length allometric slopes remained unaltered, but the
197 individual GF values were more dispersed along the slope (Fig.S3i,j); when taken as a
198 ratio (wing length/body-length), the variance was greater in the GF flies (Fig.S3h). These
199 observations indicate that gut microbes, represented by Lp^{WJL} , indeed act as a broad

200 buffer that confers phenotypic homogeneity in various physical fitness traits in a
201 genetically diverse host population.

202

203 *Lp^{WJL} conveys robustness in organ-patterning under nutritional stress*

204 We have thus far shown that *Lp^{WJL}* association confers transcriptomic stability and
205 phenotypic constancy to the developing host facing nutritional stress, in a fashion that is
206 highly reminiscent of the host's own genetic buffering mechanism. For example,
207 reducing Hsp90 activity has been shown to increase organ size variation in both plants
208 and animals[16-18]. Moreover, compromising Hsp90 can lead to morphological
209 aberrations that are otherwise "hidden"[17]. Similarly, we also found that a significant
210 fraction of the GF F₂ flies bore aberrant wing patterns such as missing margins,
211 incomplete vein formations and ectopic vein tissue (Fig.3a). The incidence of wing
212 anomalies differed according to the genotype, and females were more affected than males
213 (Fig.3b). In contrast, the most visible "defect" in their *Lp^{WJL}* associated siblings, if any,
214 were rare and hardly discernable (Fig.3a, Fig.S4a). Furthermore, gross patterning
215 anomalies were absent in the viable adults from the GF parental homozygous strains or in
216 F₂ adults reared on a standard diet (data not shown), supporting that gut microbiota likely
217 acts as a developmental canalization mechanism by suppressing the contribution of
218 cryptic genetic variation in the presence of nutritional stress. Organ patterning is a robust
219 process; changes in nutrition, humidity, temperature and crowding can alter the final
220 adult body and wing size; yet wing patterning is virtually invariant and reproducible[19].
221 Surprisingly, we found that in GF flies, constant nutritional stress can in fact unveil the
222 effects of preexisting "silent" mutations that manifest themselves as visible wing
223 patterning anomalies. Furthermore, as the patterning defects only appear in nutritionally
224 challenged F₂ flies devoid of their microbiota, we conclude that these defects reflect a
225 breach of the canalization process during developmental patterning when the hidden
226 effects of genetic variants are unlocked[20], and the gut microbiota buffers the effects of
227 these otherwise seemingly "neutral" variants to confer robustness to the canalized process
228 of organ patterning.

229 *Compromising ROS activity impairs the buffering capacity of Lp^{WJL} without affecting*
230 *bacteria growth*

231 The wing anomalies in the GF F₂ progeny highly resemble the phenotypes recently
232 reported by *Santabarbara-Ruiz* et al, who blocked ROS activity through antioxidant
233 feeding and induced regeneration defects in the wing[21]. We therefore repeated the

234 DGRP F₂ cross experiment with an additional condition by mixing the antioxidant
235 molecule N-acetylcysteine (NAC) in the diet of mono-associated flies. NAC feeding did
236 not compromise bacterial growth (Fig.S4b), but substantially diminished the buffering
237 capacity of the bacteria (Fig.4). Specifically, variation in larval size (Fig.4a),
238 developmental timing (Fig.4b and 4d) and adult emergence (Fig.4c and 4e) was
239 significantly increased in NAC-fed larvae mono-associated with *Lp*^{WJL}, to a level similar
240 to or even higher than that in GF larvae. Wing patterning anomalies were also unmasked
241 (Fig.4f). Therefore, blocking ROS activity through NAC-feeding suppresses the genetic
242 buffering effect mediated by the gut bacteria. Jones *et al.* previously reported that acute
243 exposure to *Lactobacillus plantarum* stimulates the *dNox*-dependent production of ROS
244 in larval enterocytes, and subsequently increases the expression of genes involved in the
245 Nrf2-mediated cyto-protection program[22, 23]. Future explorations are required to
246 reconcile how ROS metabolism can be integrated into the molecular dialogue between
247 the host and its intestinal microbiome to maintain robustness during development.

248

249 With a mono-association model, we unveiled that the *Drosophila* gut microbiota acts as a
250 broad genetic buffer that safeguards the host's genetic potential and confers
251 developmental robustness when confronted with nutritional stress. This function may be a
252 universal feature of beneficial microbes. In *Drosophila*, nutritional mutualism with
253 commensals is facultative and volatile by nature[7, 24, 25]. Thus, the rapid acquisition or
254 loss of particular gut community members can enable the developing host population to
255 adjust its phenotypic range in response to the changing environment. The action of
256 genetic buffering by microbiota in part invokes the concept of an "evolutionary
257 capacitance"[2], and a future challenge is to prove if increased phenotypic variation due
258 to loss of microbial buffering can be genetically assimilated in persistent nutritional
259 stress. In line with our study, recent efforts by Elgart *et al.* showed that the effect of
260 different mutant phenotypes is more pronounced in GF progeny than in their axenic
261 parents[26], suggesting potential heritability of such variation. Lastly, by showing that
262 the gut microbiota can mask the effect of cryptic genetic variation, our results may
263 contribute to resolving the long-standing enigma of incomplete penetrance and
264 expressivity in classical genetics and the "missing heritability" problem in contemporary
265 genome-wide association studies.

266

267

268 **Acknowledgments**

269 We would like to thank Benjamin Prud'homme and colleagues at ENS de Lyon for their
270 critical reading of the manuscript and valuable suggestions, the Arthro-Tools platform the
271 SFR Biosciences (UMS3444/US8) for the fly equipment and facility, the Bloomington
272 Stock Centre and VDRC for fly lines. This work was supported by an international
273 collaborative grant through the French "Agence Nationale de la Recherche" and the
274 "Fond National Suisse pour la Recherche" (ANR-15-CE14-0028-01) awarded to F.L and
275 B.D., an ERC starting grant (FP7/2007-2013-N_309704) awarded to F.L., a SystemsX.ch
276 (AgingX) Grant awarded to B.D and Institutional Support by the EPFL (B.D.). CEI was
277 funded by a Ph.D. fellowship from the Rhone-Alps region. F.L is supported by the
278 FRM/FSER foundation, the FINOVI foundation and the EMBO Young Investigator
279 Program. MBS, MF, ML, and B.D. were supported by AgingX (SystemsX.ch) and/or
280 Institutional Support by the EPFL.

281

282 **Author contributions**

283 D.M., M.B.S., B.D., and F.L. conceived the project and designed the experiments; D.M.,
284 and C.E.I., conducted all fly-related experiments; M.B.S., and M.L conducted the GWAS
285 analysis; M.B.S, M.F. and V.B prepared the libraries and conducted single-larvae
286 transcriptome analyses. P.J. conducted the multivariate statistical analyses; G.S., has
287 identified the effect of NAC on *Lp*-mediated larval phenotypes. D.M., M.B.S., B.D., and
288 F.L. analyzed the data. D.M. drafted the manuscript, D.M, M.B.S, B.D. and F.L revised
289 the paper and wrote the final draft together.

290

291

292

293 **Declaration of Interests**

294 The authors declare no competing financial interests. Correspondence and requests for
295 materials should be addressed to francois.leulier@ens-lyon.fr or bart.deplancke@epfl.ch

296

297

298

299

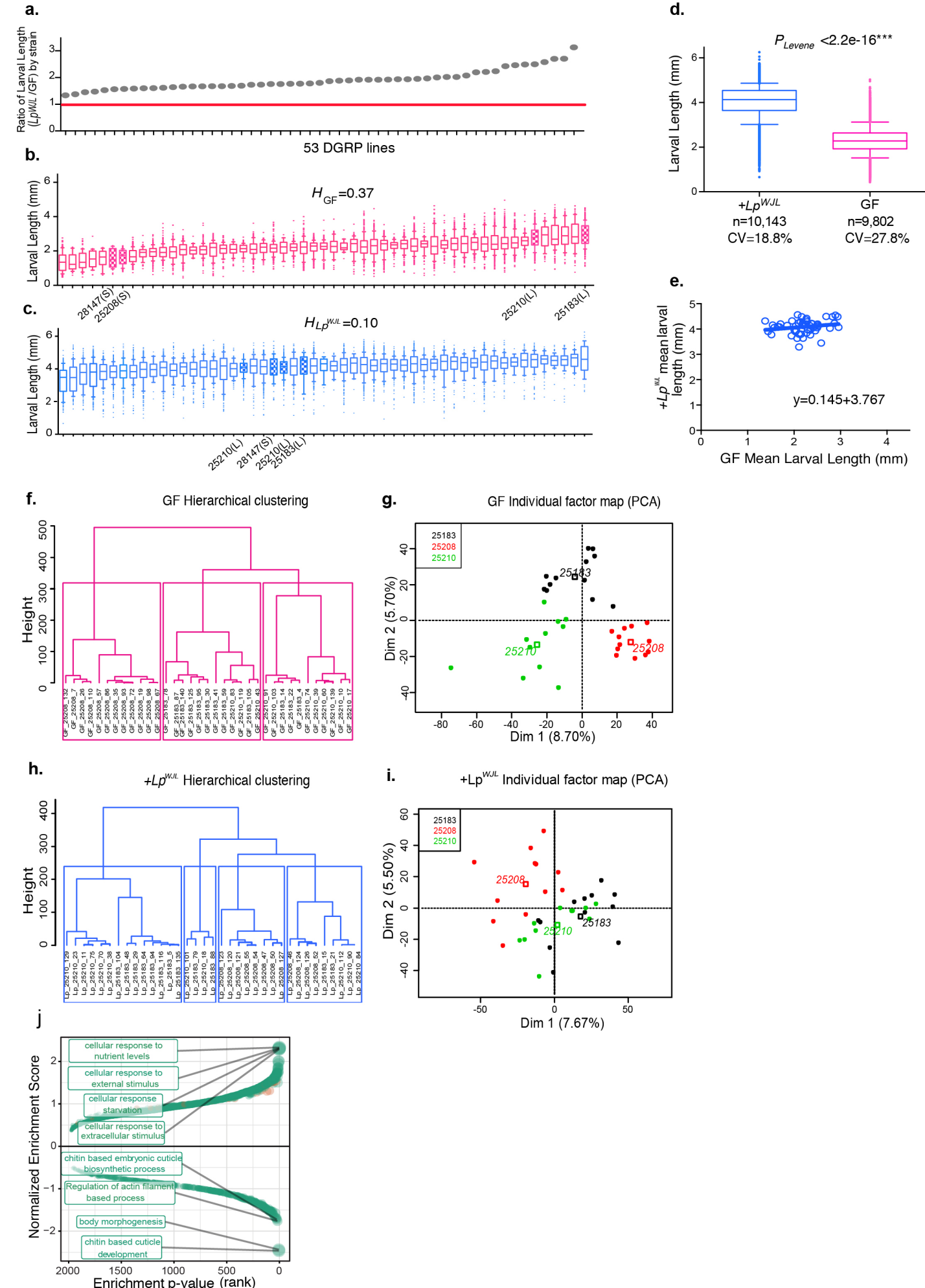


Figure 1

300 **Figure Legend**

301 **Figure 1. Mono-association with *Lp*^{WJL} buffers phenotypic and transcriptomic**
302 **variation during growth and development in the DGRP lines**

303 **a).** The ranking of larval growth gain of 53 DGRP lines was used for GWAS to uncover
304 host variants associated with growth benefits conferred by *Lp*^{WJL}. Each grey dot
305 represents the quotient of average mono-associated larval length (Figure 1c) divided by
306 the average length of GF larval length (Figure 1b) from each DGRP line on Day 7 AEL
307 (after egg lay). The red line marks the ratio of “1”, indicating that all tested DGRP lines
308 benefited from *Lp*^{WJL} presence.

309

310 **b).** and **c).** the average larval length on Day 7 AEL for each of the 53 DGRP lines (Mean
311 and 10-90 percentile. Unless specified, all box plots in this manuscript present the same
312 parameters). Each line in the box represents the average length from pooled biological
313 replicates containing all viable larvae from all experimental repeats. From each strain,
314 there are between 10-40 viable larvae in each replicate, 3 biological replicates for each
315 experiment, and 2 to 3 repeats of the experiments. **b):** germ-free (GF, pink), **c):** mono-
316 associated (+*Lp*^{WJL}, blue). Note the heritability estimate (H) in the GF population is
317 higher than in the mono-associated population (37% vs. 10%). The filled boxes denote
318 the “small (S)” and “large (L)” DGRP lines that were selected for setting up the F₂
319 crosses (see Figure S3a for crossing schemes).

320

321 **d).** Box and whiskers plots showing average larval length derived from pooled GF (pink)
322 or *Lp*^{WJL}- (blue) mono-associated DGRP lines. The coefficient of variation in the GF
323 population (27.82 %) is greater than that of the mono-association population (18.74%).
324 Error bars indicate 10 to 90th percentile. Levene’s test is used to evaluate homocedasticity
325 and Mann-Whitney test for difference in the mean ($P<0.0001****$).

326

327 **e).** Scatter plot to illustrate that *Lp*^{WJL} buffers size variation in ex-GF larvae in the DGRP
328 population. Each data point represents the intercept of the GF length and its
329 corresponding mono-associated length at Day 7 for each DGRP line. If genetic variation
330 was the only factor influencing growth in both GF and monoassociated flies, the slope of
331 the scatter plot should theoretically be 1 (Null hypothesis : slope=1, $P<0.0001$: the null
332 hypothesis is therefore rejected. A linear standard curve with an unconstrained slope was
333 used to fit the data).

334 **f.**, **g.**, **h.** and **i**). Hierarchical clustering (**f** and **h**) and PCA analyses (**g** and **i**) based on
335 individual larvae transcriptome analyses show that the samples cluster more based on
336 genotypes when germ-free (**f** and **g**, **f**: $P_{\text{genotype}}=1.048\text{e-}08$, **g**: $R^2_{\text{Dim1}}=0.73$,
337 $P_{\text{genotype}}=7.81\text{e-}10$, $R^2_{\text{Dim2}}=0.72$, $P_{\text{genotype}}=1.12\text{e-}9$,) than mono-associated (**h** and **i**, **h**:
338 $P_{\text{genotype}}=0.000263$, **i**: $R^2_{\text{Dim1}}=0.42$, $P_{\text{genotype}}=0.00017^{**}$, $R^2_{\text{Dim2}}=0.31$, P_{genotype}
339 =0.00269). A PCA followed by hierarchical clustering on principle components
340 (HCPC) was performed with the R package FactoMineR on the voom corrected read
341 counts. Correlations between the genotype variable and PCA dimensions or HCPC
342 clusters were assessed by χ^2 tests. The dots represent the different samples according to
343 genotype, and the empty squares are the calculated centers for each genotype.

344

345 **j**). Gene set enrichment analysis based on the change in standard deviation of gene
346 expression. Positive enrichment indicates gene sets that are enriched in the genes whose
347 expression level variation increases in response to Lp^{WJL} mono-association. Negative
348 gene sets are those that are enriched in the genes whose expression level variation
349 decreases in response to Lp^{WJL} mono-association. The top 4 positively and negatively
350 enriched sets are labeled. The genes whose expression levels are reduced by Lp^{WJL} mono-
351 association predominantly act in chitin biosynthesis and morphogenesis (See also FigS2.

352

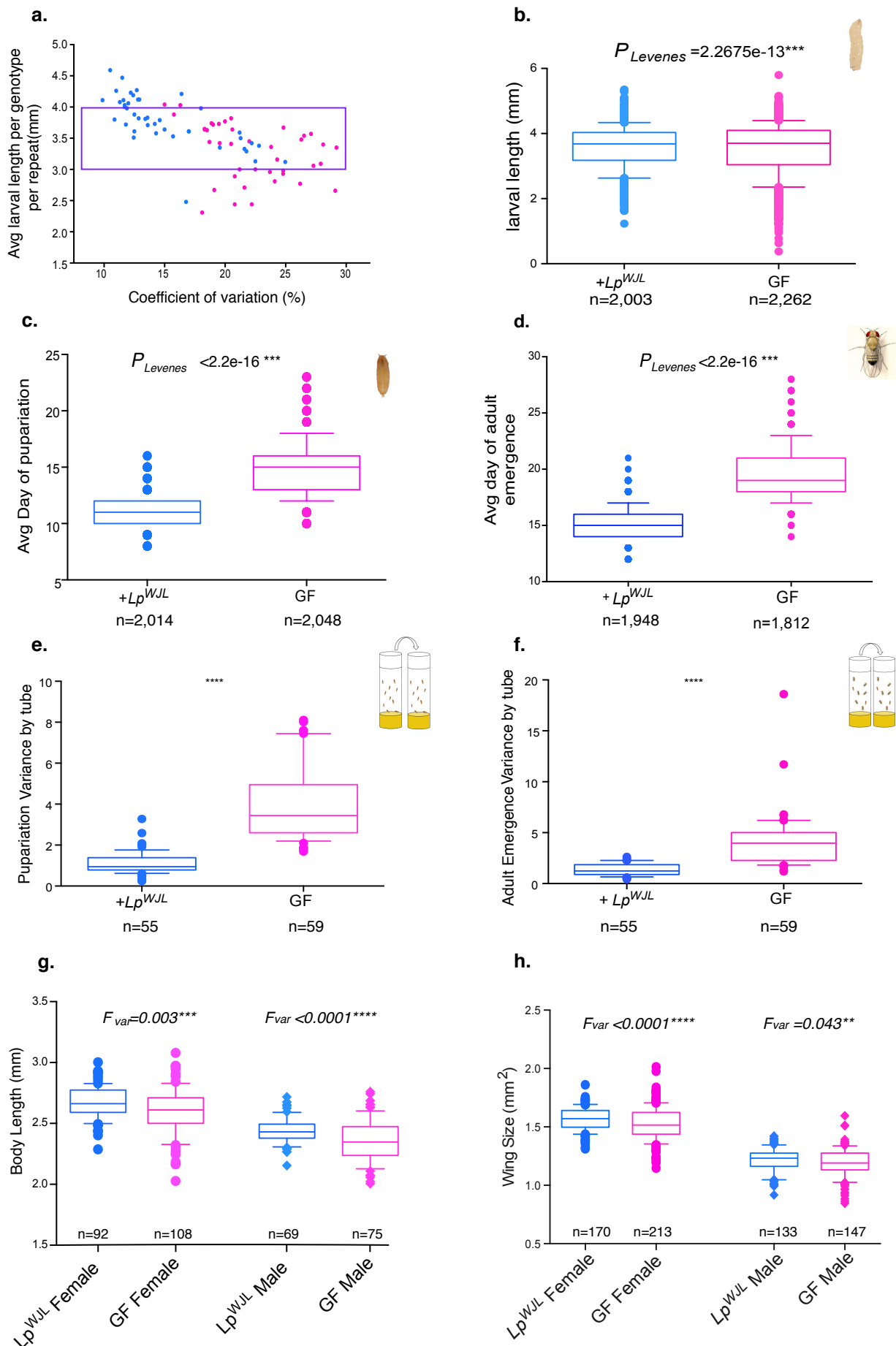


Figure 2.

353 **Figure 2. In the genetically diverse DGRP F₂ population, *Lp*^{WJL} reduces variation in**
354 **different physical fitness traits**

355 **a).** A scatter plot showing how coefficient of variation (CV) changes as a function of
356 larval length, and how such change differs in the DGRP F₂ GF (pink) and *Lp*^{WJL} mono-
357 associated (blue) populations (see Figure S3a and Methods for detailed schemes). Each
358 data point represents the intercept of a CV value and its corresponding average larval
359 length in a particular cross. Each CV, SD and average value was derived from larvae
360 measurements gathered from at least 3 biological replicates from either GF or *Lp*^{WJL}
361 mono-associated conditions. Each replicate contains 10-40 larvae. Based on multivariate
362 anova analysis, the factors affecting variants in this plot are: larval age* (P=0.053),
363 bacteria presence*** (P=3.02e-06), and larval length (P=8.27e-15***). The purple
364 bracket indicates the arbitrarily selected experiments where the average larval length for
365 each cross falls between 3mm and 4mm for size-matching purpose.

366

367 **b).** The average larval length of the F₂ progeny pooled from experiments demarcated by
368 the purple bracket in Figure 2a. While the average size is perfectly matched (GF Avg
369 Length=3.522mm, *Lp*^{WJL} Avg Length= 3.582mm, P=0.857^{ns}, Mann-Whitney test), the GF
370 population exhibits greater variation than the *Lp*^{WJL} mono-associated population
371 (Var_{GF}=0.642, CV_{GF}=22.8%, Var_{Lp}=0.427, CV_{Lp}=18.3%)

372

373 **c).** Variance and mean comparisons for the average day of pupariation for individual
374 larva in the F₂ GF and mono-associated populations. (Difference in mean P<0.0001***,
375 Mann-Whitney test, Var_{GF}= 2.42, Var_{Lp}=1.22).

376

377 **d).** Variance comparison for average day of adult emergence in the F₂ GF and mono-
378 associated populations (Difference in mean P<0.0001***, Var_{Lp}=1.84, Var_{GF}=5.27).

379

380 **e).** Box plots comparing the variances of pupariation derived from each tube containing
381 approximately 40 larvae. The average variance per tube for the GF population=3.99; the
382 average variance per tube for the *Lp*^{WJL} associated population =1.12. Var_{Lp}=0.54 ,
383 Var_{GF}=1.76. Note that these values are the “variance of variances”.

384

385 **f).** Box plots comparing the variances for adult emergence from each tube containing
386 approximately 40 larvae (Difference in mean P<0.0001***). The average variance per

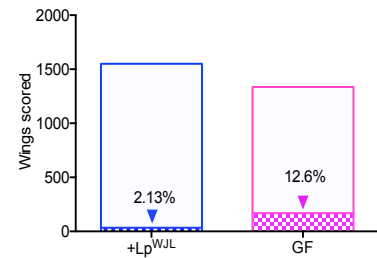
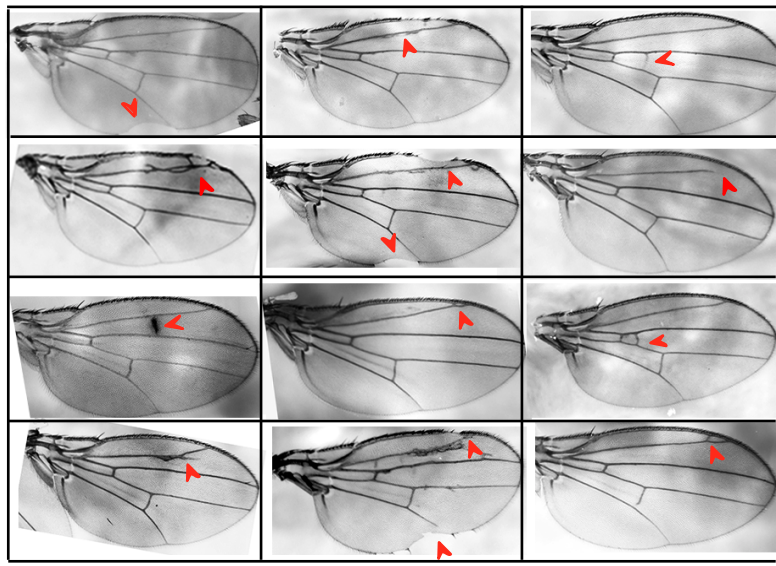
387 tube for the GF population=4.06; the average variance per tube for the Lp^{WJL} associated
388 population =1.34. For ‘variance of the variances’, $Var_{Lp}=1.33$, $Var_{GF}=4.2$.

389

390 **g).** and **h.)**In both male (lozenge) and female (circle) adults, the variances in body size (**g**).
391 the difference in mean body length: for females, $P=0.0009***$, for males, $P=0.0015**$),
392 and wing size (**h.**, the difference in mean wing area for females, $P=0.0010$, *** for males,
393 $P=0.124$, ns) are greater in the GF population than in the mono-associated population.
394 The adult data sets presented in Fig.2g and 2h and in Fig.S3g and S3h take on normal
395 distribution by D'Agostino & Pearson omnibus normality test, F variances are therefore
396 calculated and compared.

397

a.



b.

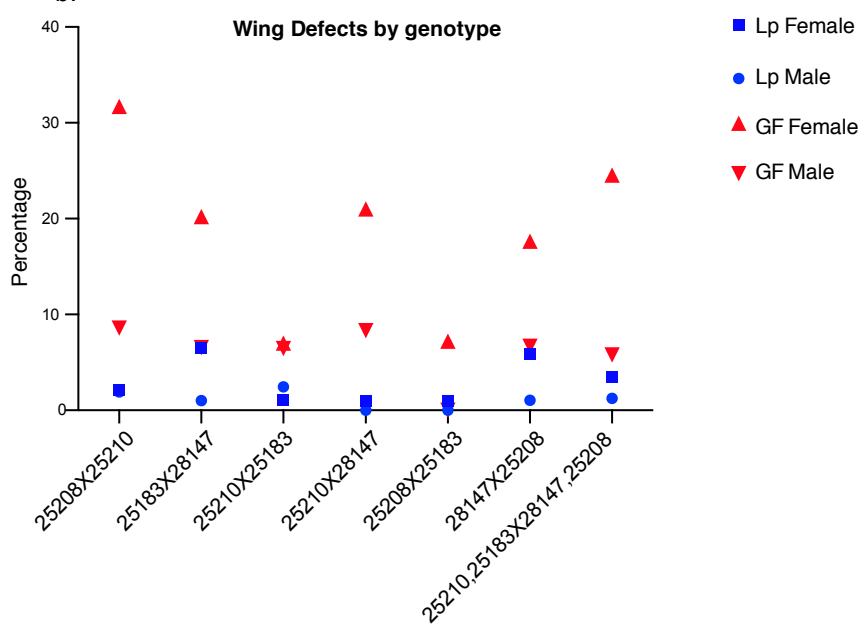


Figure 3

398 **Figure 3. In the DGRP F₂ progeny, *Lp*^{WJL} association provides robustness in wing
399 developmental patterning**

400 **a).** A compilation of representative images illustrating wing patterning anomalies in the
401 GF DGRP F₂ progeny, indicated by red arrows. The number of such patterning anomalies
402 are compiled together for GF and *Lp*^{WJL} mono-associated flies (χ^2 test, $P<0.0001^{***}$,
403 $N_{Lp}=1,551$ $N_{GF}=1,335$), and the percentage of defects are indicated inside each bar.

404

405 **b).** The incidence of wing patterning defects separated by F₂ genotypes. The Y- axis
406 denotes the percentage of wings with aberrant patterning as represented in Figure 3a..

407

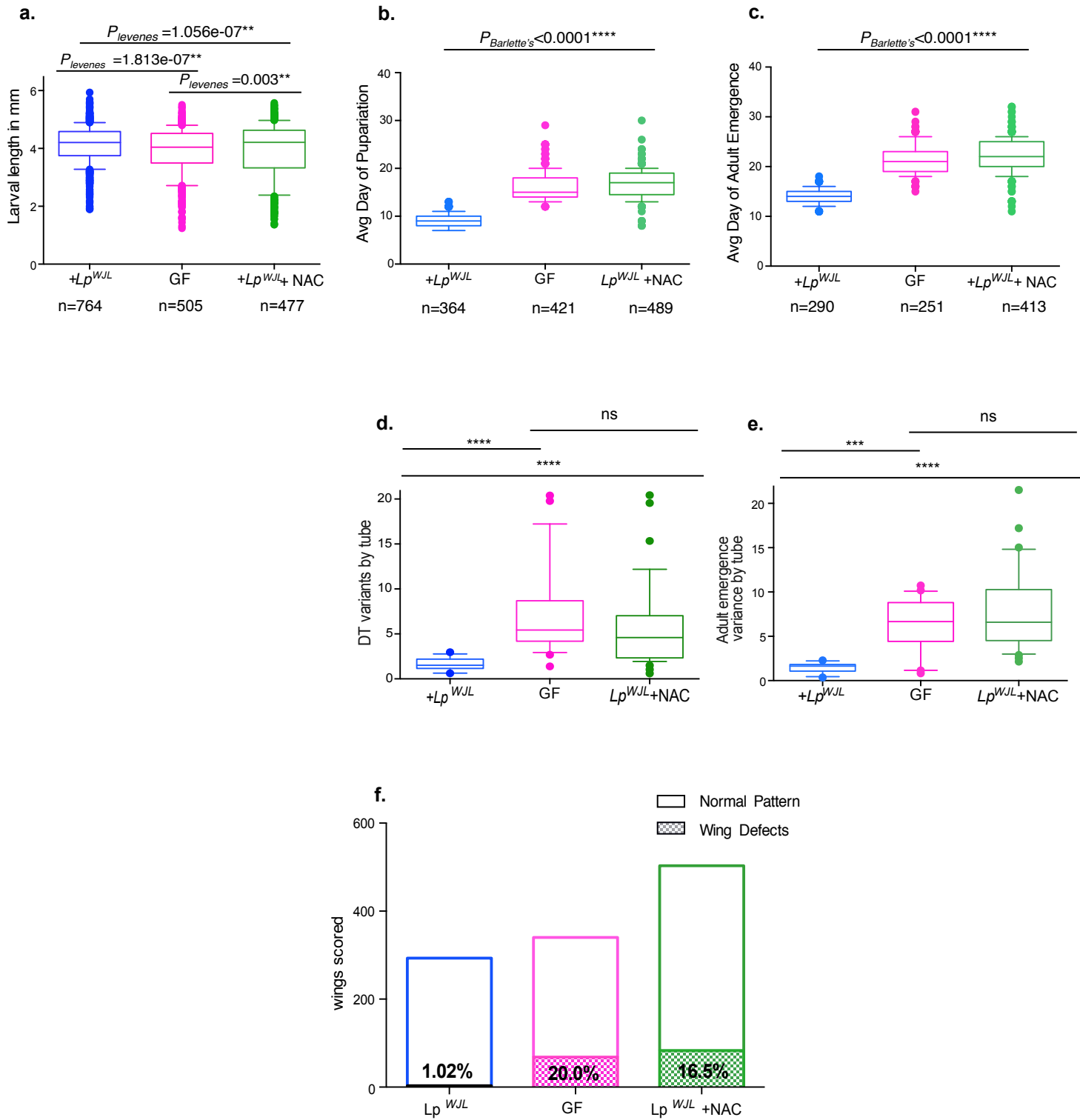


Figure 4.

408 **Figure 4. Blocking ROS activity by N-acetylcystein (NAC) compromises the *Lp*^{WJL}
409 buffering capacity**

410 **a).** In the DGRP F₂ progeny, feeding *Lp*^{WJL} mono-associated animals with food
411 supplemented with NAC increases the variances in size-matched larvae. Average Lp
412 larval size: 4.08mm; average GF larval size: 3.83mm; average *Lp*^{WJL} +NAC larval size:
413 3.94mm. There is no size difference between GF and NAC treated flies associated with
414 *Lp*^{WJL}, p=0.064. CV_{Lp}=15.8%, CV_{GF}= 20.8%; CV_{Lp+NAC}=24.0%.

415

416 **b). and c).** NAC treatment to the Lp-associated animals also increases the variances of
417 pupariation (**b**) and adult emergence (**c**). The average day to become a pupa for *Lp*^{WJL}
418 mono-associated larva: Day 8.9 (Var=2.13), for a GF larva: Day 16.1 (Var=8.27), for a
419 NAC-treated, mono-associated larva: Day 16.8 (Var=8.36). The average day for an
420 *Lp*^{WJL} mono-associated adult to emerge is: Day14.1 (Var=2.08), for a GF adult: Day 21
421 (Var= 8.3) and for a NAC-treated, mono-associated adult: Day 21.7 (Var=11.3).

422

423 **d). and e).** NAC treatment to the *Lp*^{WJL} mono-associated animals also increases the
424 among-population variances of pupariation and adult emergence. Each data point
425 represents the variance calculated based on the average day of pupariation (**d**) or adult
426 emergence (**e**) from each tube housing approximately 40 animals.

427

428 **f).** Morphological defects in the wings are also significantly increased in NAC-treated
429 mono-associated adults (D), (χ^2 test, P<0.0001***) pink: GF (N=340); Blue : +*Lp*^{WJL}
430 (N=293); Green : + *Lp*^{WJL} +NAC (N=503).

431

432 **Methods**

433 **•Fly stocks and genetic crosses**

434 Drosophila were kept at 25°C in a Panasonic Mir425 incubator with 12/12 hrs dark/light
435 cycles. Routine stocks were kept on standard laboratory diet (see below “media
436 preparation and NAC treatment”) The 53 DGRP lines were obtained from Bloomington
437 Drosophila Stock Center.

438

439 Field-collected flies were trapped with rotten tomatoes in a garden in Solaize (France)
440 and reared on a medium without chemical preservatives to minimize the modification to
441 their gut microbiota[15]. One liter of media contains 15g inactivated yeast, 25g sucrose
442 (Sigma Aldrich, ref. #84100), 80g cornmeal and 10g agar.

443

444 To generate DGRP F₂s, four DGRP lines were selected for setting up seven different
445 crosses: 25210 (RAL-859), 25183(RAL-335) are the lines with “large” larvae as germ-
446 free, and 25208(RAL-820) and 28147(RAL-158) are the line with “small” larvae as
447 germ-free (see figure legend Figure S3a).

448

449 All RNAi lines were crossed to the driver line *y,w;; tubulin-GAL80^{ts},daugtherless-*
450 *GAL4*. To minimize lethality, we dampend the *GAL4* strength by leaving the genetic
451 crosses at 25°C. The following fly strains were used: *y,w*, UAS-*dpr-6*-
452 IR(P{KK112634}VIE-260B), UAS-*CG13492*-IR, (*w¹¹¹⁸*;P{GD14825}v29390), UAS-
453 *daw*-IR(NIG #16987R-1), UAS-*sfl*-IR (*w¹¹¹⁸*; P{GD2336}v5070), UAS-*arr*-IR (*w¹¹¹⁸*;
454 P{GD2617}v4818), UAS-*rg*-IR(*w¹¹¹⁸*; P{GD8235}v17407), UAS-*bol*-IR(*w¹¹¹⁸*;
455 {GD10525}v21536), UAS-*glut1*-IR(*y^l v^l*; P{TRiP.JF03060}attP2, Bloomington 28645),
456 UAS-*CG32683*-IR (P{KK112515}VIE-260B), UAS-*CG42669*-
457 IR(*w¹¹¹⁸*;P{GD7292}v18081), UAS-*Eip75B*-IR (*w¹¹¹⁸*; P{GD1434}v44851), UAS-
458 *mCherry*-IR (*y^l v^l*; P{CaryP}attP2), VDRC GD control (VDRC ID60000).

459

460 **•GWAS and data computing of heritability indice**

461 To calculate heritability, we estimated variance components using a random effects
462 model using the lme4 R package[27]. Strain and experiment date were treated as random
463 effects, and the heritability was calculated as VA/(VA+VD+VR), where VA is the
464 additive genetic variance, and is equal to twice the Strain variance, VD is the experiment
465 date variance, and VR is the residual variance. For the GWAS, we used the online tool

466 specifically designed for the DGRPs (<http://dgrp2.gnets.ncsu.edu/>)[28, 29]. The
467 Manhattan and QQ-plots were generated using R.

468

469 **•Single larva transcriptome analysis**

470 *RNA extraction from single larvae:* Larvae were handpicked under the microscope using
471 forceps and transferred to Eppendorf tubes filled with 0.1 uL of beads and 350 uL of
472 Trizol. The samples were then homogenized using a Precellys 24 Tissue Homogenizer at
473 6000 rpm for 30 seconds. After homogenization, the samples were transferred to liquid
474 nitrogen for flash freezing and stored at -80°C. For RNA extraction, samples were
475 thawed on ice, 350 uL of 100% Ethanol was then added to each sample before
476 homogenizing again with the same parameters. Direct-zol™ RNA Miniprep R2056 Kit
477 was used to extract RNA with these modifications: DNase I treatment was skipped; after
478 the RNA Wash step, an extra 2 min centrifugation step was added to remove residue
479 wash. Lastly, the sample was eluted in 10 uL of water, incubated at room temperature for
480 2 min and then spun for 2 min to collect RNA. RNA was transferred to a low-binding 96
481 well plate and stored at -70°C.

482

483 *RNA-sequencing:* We prepared the libraries using the BRB-seq protocol and sequenced
484 them using an Illumina NextSeq 500[11]. Reads from the BRB-seq protocol generates
485 two fastq files: R1 containing barcodes and UMIs and R2 containing the read sequences.
486 R2 fastq file was first trimmed for removing BRB-seq-specific adapter and polyA
487 sequences using the BRB-seqTools v1.0 suite (available at
488 <http://github.com/DeplanckeLab/BRB-seqTools>). We then aligned the trimmed reads to
489 the Ensembl r78 gene annotation of the dm3 genome mixed with the *Lactobacillus*
490 *Plantarum* WJL genome using STAR (Version 2.5.3a)[30], with default parameters (and
491 extra "--outFilterMultimapNmax 1" parameter for completely removing multiple mapped
492 reads). Then, using the BRB-seqTools v1.0 suite (available at
493 <http://github.com/DeplanckeLab/BRB-seqTools>), we performed simultaneously the
494 sample demultiplexing, and the count of reads per gene from the R1 FASTQ and the
495 aligned R2 BAM files. This generated the count matrix that was used for further analyses.
496 Genes were retained in the analysis if they had more than 10 reads in more than 50
497 samples. The data was subsequently transformed using the voom method. Differential
498 expression was performed using the R Limma package[31, 32]. Genes with a log₂ fold
499 change greater than 2 and a Benjamini-Hochberg adjusted P-value less than 0.05 were

500 considered differentially expressed. Since the library preparation was performed in two
501 plates, hence introducing a batch effect, we used the duplicateCorrelation function and
502 included the batch as a blocking variable. Prior to PCA analysis and standard deviation
503 calculations, we removed the batch effect using the removeBatchEffects function and
504 then used the princomp function. We used the cluster profiler package to perform GSEA
505 analyses. The gmt file containing the gene ontology annotations was obtained from
506 GO2MSIG data. Specifically, we used the high quality GO annotations for *Drosophila*
507 *melanogaster*. For each GSEA analysis, we used 100,000 permutations to obtain adjusted
508 p-values and only included gene set sizes to between 6 and 1000 genes. The raw
509 expression data has been deposited in ArrayExpress (accession number: E-MTAB-6518)
510

511 **RNA-sequencing:** We prepared the libraries using the BRB-seq protocol and sequenced
512 them using an Illumina NextSeq 500[11]. Reads from the BRB-seq protocol generates
513 two fastq files: R1 containing barcodes and UMIs and R2 containing the read sequences.
514 R2 fastq file was first trimmed for removing BRB-seq-specific adapter and polyA
515 sequences using the BRB-seqTools v1.0 suite (available at
516 <http://github.com/DeplanckeLab/BRB-seqTools>). We then aligned the trimmed reads to
517 the Ensembl r78 gene annotation of the dm3 genome mixed with the *Lactobacillus*
518 *Plantarum* WJL genome using STAR (Version 2.5.3a)[30], with default parameters (and
519 extra "--outFilterMultimapNmax 1" parameter for completely removing multiple mapped
520 reads). Then, using the BRB-seqTools v1.0 suite (available at
521 <http://github.com/DeplanckeLab/BRB-seqTools>), we performed simultaneously the
522 sample demultiplexing, and the count of reads per gene from the R1 FASTQ and the
523 aligned R2 BAM files. This generated the count matrix that was used for further analyses.
524 The data was subsequently transformed using the voom method and analyzed using the R
525 Limma package[31, 32].
526

527 The raw expression data of BRB-Seq has been deposited in ArrayExpress (accession
528 number: E-MTAB-6518)
529
530
531
532
533

534 **•The making and maintenance of germ-free flies**

535 Axenic flies were generated by dechorionating embryos with 50% household bleach for
536 five minutes; eggs were then washed in successive 70% ethanol and sterile distilled water
537 for three minutes each. After washing, eggs were transferred to tubes containing standard
538 diet and a cocktail of antibiotics containing 50 μ g/mL ampicillin, 50 μ g/mL kanamycin,
539 15 μ g/mL erythromycin, 50 μ g/mL tetracyclin for stock maintenance. Axeny was
540 routinely verified by plating larvae and adult lysates on LB and MRS plates. For
541 experiments food without antibiotics was used.

542

543 **•Media preparation and NAC treatment**

544 Standard laboratory fly food consists of 50g/L inactivated yeast (SpringalineTM), 80g/L
545 cornmeal, 7.14g/L agar, 5.12g/L Moldex (Sigma M-50109) and 0.4% propionic acid.
546 Where applicable, experiments comparing variations in larval size, developmental timing,
547 adult emergence were performed on diet with 6g or 8g inactivated yeast per liter of media
548 while keeping the same concentrations for the other ingredients. Where appropriate,
549 1.7g/L of N-Acetylcysteine (SigmaA7250-25g) was added to the low-protein diet.

550

551 **•Larval Length Measurement**

552 All live *Drosophila* larvae were collected from each nutritive cap containing low yeast
553 diet by temporary immersion in sterile PBS, transferred on a microscopy slide, killed with
554 a short pulse of heat (5 sec at 90°C), mounted with 80% glycerol/PBS. The images were
555 taken with the Leica stereomicroscope M205FA and the lengths of individual larvae were
556 measured using ImageJ software[33]. For each DGRP strain and each cross and/or
557 condition, at least three biological replicates were generated.

558

559 **•Developmental timing and Adult emergence**

560 Developmental timing and adult emergence of the flies were quantified by counting the
561 number of individuals appearing every 24 hours until the last pupa/adult emerges. Each
562 animal is assigned to the number that corresponds to the day it appeared, and the
563 population mean and variance were calculated based on the cumulative numbers.

564

565 **•Adult trait measurements**

566 2-3 days old adult flies were anesthetized with CO₂ and immersed in 70% ethanol, and
567 the individual body and its corresponding organ (wing and eye) were imaged under a

568 Leica M205 stereomicroscope. Specifically, the adult body length was measured from the
569 top of the head to the tip of the abdomen. The eye area was measured by manually tracing
570 the circumference of both eyes. The wings were gently nipped at the base of the hinge
571 and imaged, and the area was measured by tracing the edge of the wing. All images were
572 taken measured using ImageJ software

573

574 **•Bacteria culture and mono-association**

575 For each mono-association experiment, *Lp^{WJL}* [34] was grown in Man, Rogosa and
576 Sharpe (MRS) medium (Difco, ref. #288110) over-night at 37°C, and diluted to O.D.=0.5
577 the next morning to inoculate 40 freshly laid eggs on a 55mm petri dish or standard
578 28mm tubes containing fly food of low yeast content. The inoculum corresponds to about
579 5x10⁷ CFUs. Equal volume of sterile PBS was spread on control axenic eggs.

580

581 To contaminate the garden-collected flies with their own microbiota, eggs were
582 dechorionated and directly seeded onto appropriate food caps. Sterile PBS was used to
583 wash the side of the bottles where the adult wild flies were raised to recover more fecal
584 content, and 300 ul of the wash was inoculated to the dechorionated eggs. For GF control,
585 300 ul of sterile PBS was used to inoculate the dechorionated eggs. The microbial
586 composition of this microbiota can be founded here[15].

587

588 **•Bacteria niche load**

589 Five to six 24 hour old germ-free larvae were collected from the low-protein diet food
590 cap and transferred to a microtube containing 400ul of low-protein diet, and inoculated
591 with 50ul of *Lp^{WJL}* of 0.5 O.D.. On the day of harvest, ~0.75-1mm glass micro-beads and
592 900µl PBS were added to each microtube and the entire content of the tube was
593 homogenized with the Precellys-24 tissue homogenizer (Bertin Technologies). Lysate
594 dilutions (in PBS) are plated on MRS agar with Easyspiral automatic plater
595 (Intersciences). The MRS agar plates were incubated for 24h at 37°C. The CFU/ml count
596 was calculated based on the readings by the automatic colony counter Scan1200
597 (Intersciences)

598

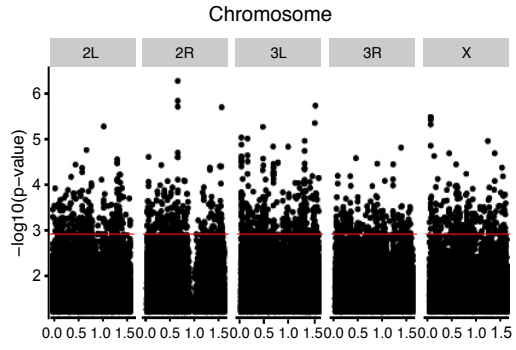
599 **•Statistical Analysis and data representation**

600 GraphPad Prism software version 6.0f for Macintosh (GraphPad Software, La Jolla
601 California USA, www.graphpad.com) was used to compare GF and *Lp^{WJL}*-associated

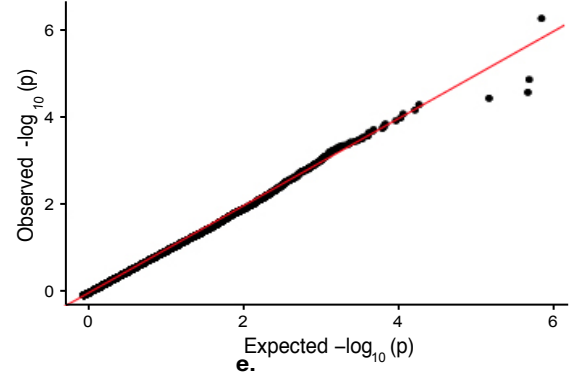
602 conditions for larval length, developmental timing, adult emergence, allometry and linear
603 regression analysis for the buffering effect. For small samples with less than 10 data
604 points, nonparametric analysis was conducted. R-studio was used to conduct Levene's
605 test and multivariate analyses. For all experiments, the p-values were reported on the
606 corresponding figure panels only when inferior to 0.05.

607

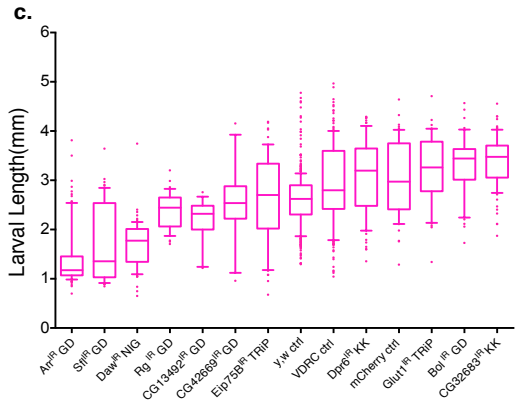
a.



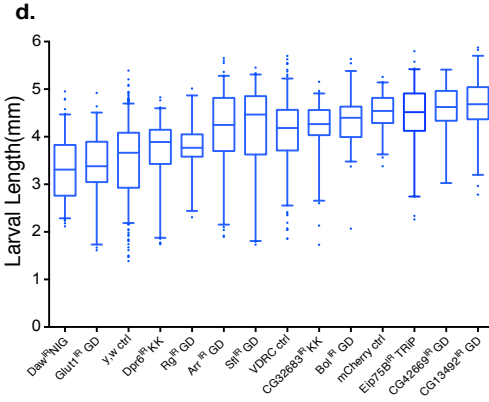
b.



c.



d.



e.

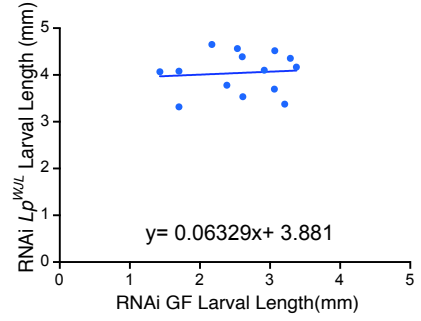


Figure S1

608 **Figure S1.**

609 **a).** Manhattan plot of the GWAS performed on the average larval length fold change per
610 DGRP line. We used the DGRP2 website for the association analysis
611 (<http://dgrp2.gnets.ncsu.edu/>)[28, 29].

612

613 **b).** Quantile-Quantile plot of the GWAS results.

614

615 **c). and d).** Box and whiskers plots illustrating the effect of RNAi knockdown on larval
616 length on day 7 AEL. Each bar represents the average length from pooled 3-5 biological
617 replicates from either condition, with 15-40 larvae in each replicate. **c:** GF. **d:** Lp^{WJL} .
618 Three different control knockdowns were used: one control fly strain recommended by
619 VDRC for RNAi constructs obtained from VDRC, one control strain (against mCherry)
620 recommended by the Harvard TRiP collection, and the *y,w* strain from Bloomington. All
621 control and RNAi strains were crossed to *y,w*; *tubulin-GAL80^{ts},daugtherless-GAL4*.
622 “GD” refers to the VDRC RNAi GD collection. “KK” refers to the VDRC RNAi KK
623 collection. For specific genotypes, refer to Material and Methods.

624

625 **e).** Lp^{WJL} also buffers growth differences in various RNAi knock-down experiments for
626 each of the candidate genes. Each data point represents the intercept of the GF length and
627 its corresponding mono-associated length at Day 7 for the RNAi knockdown experiment.
628 (Null hypothesis: Slope =1. $P=0.0008$, the null hypothesis is therefore rejected). These
629 data points were fitted into an unconstraint model. For specific genotypes, we refer to
630 Table 2 and Methods.

631

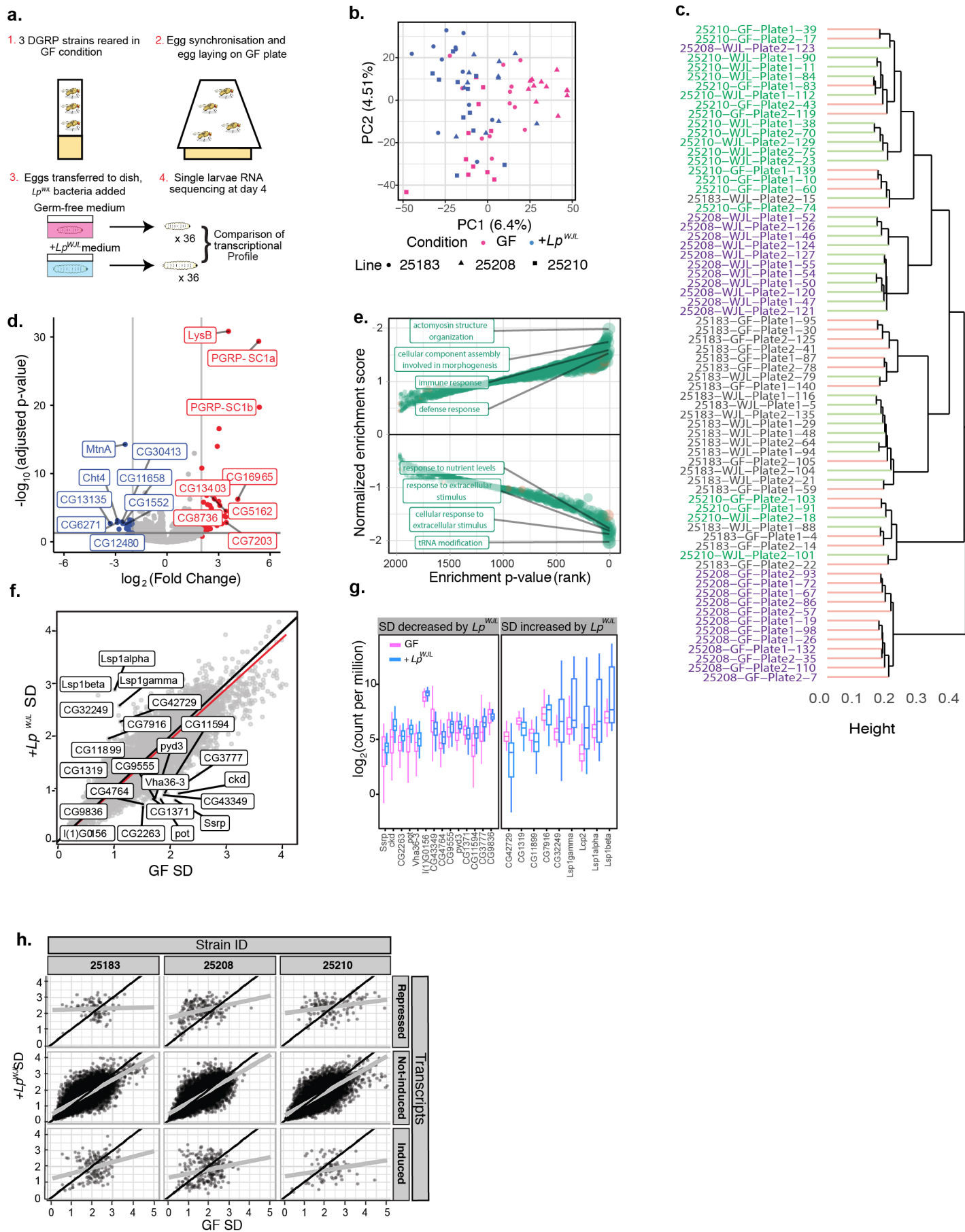


Figure S2

632 **Figure S2**

633 **a).** Experimental setup to perform BRB-seq-based transcriptomics on individual larvae.

634 Flies from three DGRP strains were reared in GF conditions. Egg-laying was
635 synchronized and embryos were transferred to food caps: three left germ-free (1X PBS)
636 and three inoculated with *Lp^{WJL}* (OD 0.5 in 1x PBS). At day 4, single larvae were
637 collected from all plates, RNA extraction and RNA sequencing were performed. In sum,
638 12 larvae were collected per line for each condition, totaling 72 single larval
639 transcriptomes.

640

641 **b).** Principal component plot of the corrected expression data after batch correction.

642

643 **c).** Hierarchical clustering of the transcriptomic data using the Ward's method. A batch
644 effect of plate was corrected prior to clustering. The genotypes are color coded (Green:
645 25210, violet: 25208, black: 25183). The red “branches” of the cluster represent GF
646 samples, and green ones represent mono-associated samples.

647

648 **d).** The observed effect of *Lp^{WJL}* mono-association on gene expression is consistent with
649 our previous findings, thus validating our transcriptome approach on individual larvae.
650 The horizontal grey line represents the 0.05 FDR-corrected p-value threshold. The
651 vertical lines are the -2 and 2 log2 (Fold Change) thresholds. Genes in red, such as *LysB*,
652 *PGRP-SC1a&b* are significantly up-regulated; they are predominantly involved in host
653 immune and defense response (see also S1e); genes in blue are significantly down-
654 regulated. Several representative genes of the top differentially regulated genes from each
655 category are highlighted.

656

657 **e).** Gene set enrichment analysis on biological process gene ontology (GO) terms based
658 on the effect of *Lp^{WJL}* mono-association. Gene sets in orange were derived from
659 GLAD[35], whereas green gene sets were extracted from GO2MSIG[36]. Note that
660 “immune response”, “defense response” and “cellular component assembly involved in
661 morphogenesis” are among the most up-regulated gene sets by mono-association (top
662 panel), and genes associated to “response to nutrient levels”, “cellular response to
663 starvation” and “t-RNA modification” were down-regulated by *Lp^{WJL}* (bottom panel).
664 Therefore, both microbe detection and nutrient adaptation drive the most significantly
665 detected transcriptomic changes in mono-associated larvae.

666 **f).** Scatterplot of the standard deviation in expression level of each gene in the GF and
667 Lp^{WJL} mono-associated condition. The black line represents the theoretical slope of 1 and
668 intercept 0. The red line is a linear fit of the points. Labelled genes show the highest
669 relative change in their standard deviation, as determined by the absolute value of
670 $\log_2(\text{SD}_{Lp^{WJL}}/\text{SD}_{\text{GF}})$.

671

672 **g).** Box and whiskers plots showing the expression levels of genes with high relative
673 change in standard deviation, regardless whether the genes themselves were up- or down-
674 regulated. Among the genes whose expression variation decreased the most upon Lp^{WJL}
675 association are *Ssrp*, a member of the FACT chromatin complex[37, 38], and many
676 cuticle-related proteins (left panel), whereas for genes induced by Lp^{WJL} , such as Larval
677 serum proteins (*Lsp1s*), more expression variation is detected (right panel).

678

679 **h).** Scatterplots of standard deviations of each gene calculated by genotype. Genes were
680 faceted by how their differential expression alters within each strain in both GF and Lp^{WJL}
681 mono-associated conditions: repressed (top panel), non-induced (middle panel) and
682 induced (bottom panel). The black lines represent the theoretical slope of 1 and intercepts
683 0, the grey lines are the linear fit to the data. Since transcripts specifically modulated by
684 Lp^{WJL} tend to have incomparable SD, we assessed GO enrichment only on non-
685 differentially expressed genes (**see Fig.1j**)

686

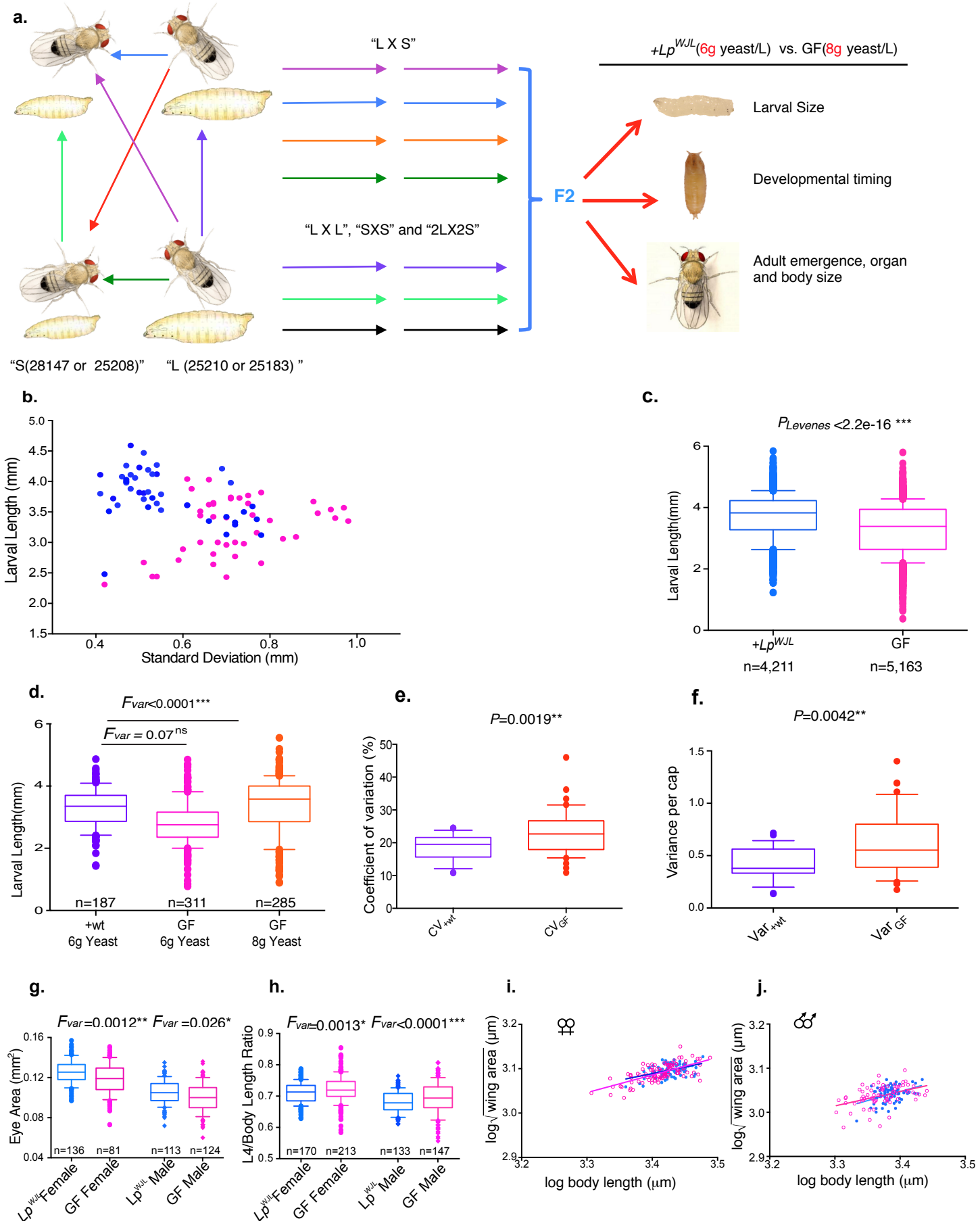


Figure S3

687 **Figure S3**

688 **a).** A diagram illustrating DGRP crosses to generate the F₂ generation for studying
689 variation in larval size, pupariation and adult emergence. 25210 (RAL-859), 25183(RAL-
690 335) are the lines with the “large” (“L”) larvae as germ-free, and 25208(RAL-820) and
691 28147(RAL-158) are the lines with the “small” larvae as germ-free (“S”). Seven possible
692 crosses are set up: 25210X25183 (“LXL”), 25208X28147(“SXS”), 25210X25208,
693 25183X25208, 25210X28147, 25183X28147 are the four “LXS” crosses, and 25183 and
694 25210 X 25208 and 28147 is the “2L X 2S” cross.

695

696 **b).** A scatter plot showing how standard deviation (SD) changes as a function of larval
697 length, and how such change differs in the DGRP F₂ GF (pink) and *Lp*^{WJL} mono-
698 associated (blue) populations (see also Figure 2a and Methods for detailed schemes).
699 Each data point represents the intercept of an SD value and its corresponding average
700 larval length in a particular cross. Each SD and average length was derived from larvae
701 measurements gathered from at least 3 biological replicates from either GF or *Lp*^{WJL}
702 mono-associated conditions. Each replicate contains 10-40 larvae.

703

704 **c).** Box and Whisker graph illustrating the average length and standard deviation from
705 pooled GF (pink) and *Lp*^{WJL} mono-associated DGRP (blue) F2 larvae, pooled from all the
706 crosses in all three different repeats (Average GF larval length: 3.29mm; average Lp
707 mono-associated larval length: 3.71mm; CV_{GF}=24.9%, CV_{Lp}=19.5%).

708

709 **d).** One representative experiment showing that re-associating the field-collected flies
710 tends to buffer the variability in body length in size-matched larvae. The purple box
711 represents body length from wild larvae grown on media contaminated with their
712 untreated parents’ fecal matter. Average GF larval length grown on 6g/L yeast media:
713 2.81mm; average GF larval length grown on 8g/L yeast media: 3.36mm: average re-
714 associated larval length (“+wt”): 3.07 mm; P= 0.338. CV_{GF} (6g/L, pink)= 24.9%, CV_{GF}
715 (8g/L, orange)= 27.0%, CV_{wt} (purple)= 18.9%.

716

717 **e. and f).** The compiled CV values (e.) and variances (f.) derived from each low-yeast
718 cap containing 40~50 field-collected larvae. The average CV and variance are lower in
719 the population re-associated with its own microbiota (purple) than in the GF population
720 (orange)

721 **g).** In both male (lozenge) and female (circle) adults, the variances in eye size are greater
722 in GF F₂ progeny. The difference in mean eye area, for females P<0.0001***; for males,
723 P=0.0013**.

724

725 **h).** The length of the L4 vein in the wing is used as a proxy of the wing length. In the
726 accumulated ratios of wing length over body length, the variances are greater in the GF
727 flies (The difference in average L4/ body length, for females P<0.0028**; for males,
728 P=0.02*).

729

730 **i). and j).** Scatter plots illustrating the allometric relationship between wing area and
731 body size in female (i) and male (j) DGRP F₂ adults. Pink open circles: GF, blue filled
732 circles: *Lp*^{WJL}. Each line represents the allometric slope of the data points shown by the
733 same color. Either in males or females, there is no difference in allometric slope between
734 the GF and mono-associated population. For GF females, $Y_{GF} = 0.3963*X + 1.738$,
735 95%C.I.= 0.3117 to 0.4810; for *Lp*^{WJL} females, $Y_{Lp} = 0.2978*X + 2.076$, 95%C.I.=
736 0,1785 to 0,4172, P=0.203, n.s ; for GF males, $Y_{GF} = 0.3261*X + 1.939$, 95%C.I.=
737 0.1725 to 0.4796 ; for *Lp*^{WJL} males, $Y_{Lp}= 0.4141*X + 1.639$, 95% C.I. =0.1842 to 0.6439,
738 P=0.55, ns.

739

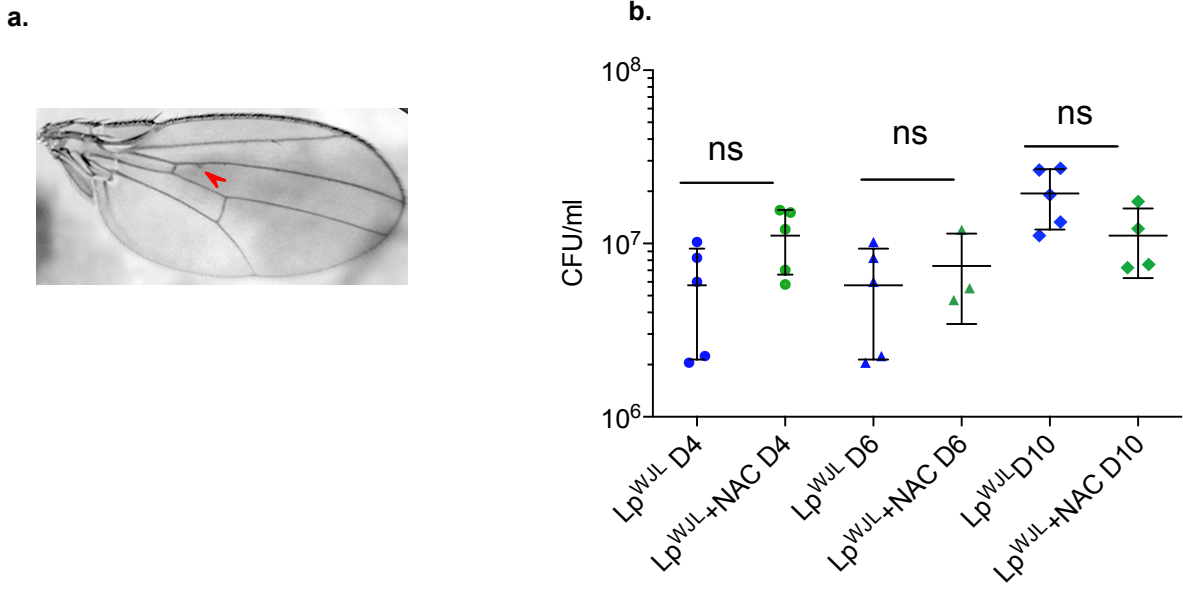


Figure S4

740 **Figure S4**

741 a.) An image of a wing of an Lp^{WJL} adult is shown, as a representation of the most visible
742 “defect” ever observed in mono-associated adults. Red arrow points to the subtle vein
743 tissue thickening. We included these as “defects” in the Lp^{WJL} F₂ population in the
744 analyses presented in Figure 3a, 3b, and 4f.

745

746 **b).** Bacterial niche load (NL) evolution (“Niche” is defined as the substrate with both
747 larvae and bacteria present) during the course of larval development with Lp^{WJL} with or
748 without NAC treatment (Day 4, Day 6 and Day 10).

749

TableS1. Average D7 larvae length for individual DGRP lines (Related to Figure1)

DGRP Lines	GF* Length(mm)	GF SD*(mm)	Lp ^{WJL *} Length(mm)	Lp ^{WJL} SD(mm)	Lp ^{WJL} /GF Ratio
25174	2.193	0.584	3.637	0.895	1.658
25175	2.693	0.687	4.496	0.659	1.670
25176	1.443	0.536	3.903	0.648	2.704
25180	2.151	0.454	3.795	0.635	1.764
25181	2.374	0.824	4.224	0.946	1.779
25182	2.108	0.451	3.293	0.859	1.562
25183	2.961	0.657	4.066	0.548	1.373
25184	1.957	0.53	4.323	0.587	2.209
25185	2.459	0.681	3.93	0.722	1.598
25186	2.278	0.667	4.289	0.803	1.883
25187	2.109	0.479	3.798	0.744	1.801
25188	2.253	0.421	4.202	0.786	1.865
25189	2.586	0.393	3.448	0.876	1.333
25190	2.292	0.512	3.976	0.941	1.735
25191	2.348	0.428	3.953	0.797	1.684
25192	2.194	0.401	4.145	0.731	1.889
25193	2.414	0.582	4.05	0.782	1.678
25194	2.506	0.558	4.195	0.508	1.674
25195	2.07	0.402	3.635	0.867	1.756
25197	1.944	0.397	3.73	0.734	1.919
25198	2.051	0.394	3.936	0.673	1.919
25199	1.514	0.524	3.78	0.753	2.497
25200	2.869	0.752	4.227	0.605	1.473
25201	2.182	0.347	4.186	0.601	1.918
25202	2.273	0.639	3.85	0.792	1.694
25203	1.541	0.513	4.158	0.755	2.698
25204	1.686	0.678	4.088	0.774	2.425
25205	2.351	0.567	3.77	0.606	1.604
25206	2.5	0.643	4.173	0.619	1.669
25207	2.028	0.481	3.896	0.811	1.921
25208	1.649	0.443	4.103	0.947	2.488
25209	2.187	0.67	4.232	0.819	1.935
25210	2.772	0.633	4.03	0.466	1.454
25445	2.01	0.468	3.956	0.668	1.968
25744	2.097	0.34	4.235	0.666	2.020
25745	2.501	0.612	4.051	0.599	1.620
28132	2.828	0.684	4.485	0.534	1.586
28134	1.854	0.383	4.144	0.479	2.235
28136	1.707	0.415	4.204	0.548	2.463
28138	1.38	0.487	4.318	0.693	3.129
28142	2.938	0.836	4.487	0.489	1.527
28146	2.077	0.36	4.564	0.915	2.197
28147	1.575	0.552	4.061	0.728	2.578
28153	2.298	0.329	3.97	0.541	1.728
28154	2.256	0.339	4.365	0.482	1.935
28160	2.51	0.662	4.118	0.714	1.640
28164	2.394	0.448	4.207	0.584	1.757
28166	2.163	0.402	4.489	0.642	2.075
28173	2.039	0.309	4.122	0.697	2.022
28192	2.141	0.506	4.286	0.659	2.002
28194	2.269	0.565	4.424	0.72	1.950
28197	2.89	0.742	4.547	0.519	1.573
28208	2.339	0.438	4.14	0.705	1.767

Table S1 (Continued)

*GF: germ-free

**Lp^{WJL}*: *Lactobacillus plantarum*, stain name: WJL

*SD: standard deviation

Table S2 . Variants associated with the growth benefits conferred by *Lactobacillus plantarum* (*Lp^{WJL}*) (Related to Figure S1)

Variants	R ²	P-value	Minor allele	Major allele	Ref* allele	MAF*	Variant Class	Molecular and cellular functions
CG13492	46.46%	1.23E-06	C	T	C	0.245	intron	Unknown
	45.81%	4.526E-07	T	A	T	0.244		
	45.56%	1.65E-06	G	A	G	0.25		
CG32683	39.04%	2.76E-06	A	T	T	0.2453	Intron/downstream	Unknown, arrestin-like
	39.04%	2.76E-06	A	C	C	0.2453		
	29.32%	4.03E-06	T	A	A	0.22		
	29.07%	3.19E-06	T	G	G	0.2245		
	29.80%	1.17E-05	CTGTTG	C	C	0.283		
CG33269	35.58%	8.21e-06	G	A	A	0.14	Intergenic	Unknown
dpr6	33.06%	2.94E-05	A	T	T	0.1224	Intron	Immunoglobulin-like domain; sensory perception of chemical stimulus
	21.34%	7.77E-06	A	G	G	0.08		
Eip75B	32.65%	1.22E-05	C	T	C	0.1176	Intron	Nuclear hormone receptor, ecdysone response, antimicrobial humoral response
rg	32.14%	9.25E-06	G	A	G	0.4	Intron	PKA-binding, cone cell differentiation, mushroom body development, olfactory learning
sfl	27.37%	9.18E-06	G	T	T	0.4706	Intron	heparan sulfate proteoglycans (HSPGs) biosynthesis/wg morphogen diffusion
CG42669	26.66%	1.23E-05	A	G	G	0.1373	Intron	Supervillin, actin-binding
bol	25.07%	3.76E-06	C	T	T	0.2	3'UTR	RNA binding protein. Role in meiotic entry and germline differentiation
CR43427, lncRNA566	23.7%	4.53E-06	G	T	T	0.3269	intergenic	Unknown, lncRNA
daw	15.1%	4.45E-06	T	C	C	0.1837	Synonymous substitution	TGF-β ligand: growth; regulation of insulin secretion
arr	14.68%	1.69E-06	G	C	C	0.1875	intron	wnt protein binding/canonical wnt pathway
glut1	11.14%	1.56E-06	G	T	T	0.2245	intron	General glucose/sugar transporter

*MAF: minor allele frequency in the 53 DGRP lines

*Ref allele: allele info derived from BDGP (Berkeley Drosophila Genome Project)

R² reflects effect size

Table S3. Individual larval transcriptome sample list (Related to Figure S2)

SampleID	Genotype	Treatment	Plate	Individual	Well_Row	Well_Column	TotalReads	Timepoint
GF-d4-Plate1-25183-4	25183	GF	Plate1	4	D	1	3374679	d4
WJL-d4-Plate1-25183-5	25183	WJL	Plate1	5	E	2	4323699	d4
GF-d4-Plate2-25208-7	25208	GF	Plate2	7	E	9	1537636	d4
GF-d4-Plate1-25210-10	25210	GF	Plate1	10	D	5	3969828	d4
WJL-d4-Plate1-25210-11	25210	WJL	Plate1	11	E	6	5131500	d4
GF-d4-Plate2-25183-14	25183	GF	Plate2	14	E	1	3307084	d4
WJL-d4-Plate2-25183-15	25183	WJL	Plate2	15	D	2	2816461	d4
GF-d4-Plate2-25210-17	25210	GF	Plate2	17	E	5	5063082	d4
WJL-d4-Plate2-25210-18	25210	WJL	Plate2	18	D	6	4162852	d4
GF-d4-Plate1-25208-19	25208	GF	Plate1	19	D	9	2459570	d4
WJL-d4-Plate2-25183-21	25183	WJL	Plate2	21	E	2	2399808	d4
GF-d4-Plate2-25183-22	25183	GF	Plate2	22	D	1	4448517	d4
WJL-d4-Plate2-25210-23	25210	WJL	Plate2	23	E	6	4508569	d4
GF-d4-Plate1-25208-26	25208	GF	Plate1	26	E	9	2085683	d4
WJL-d4-Plate1-25183-29	25183	WJL	Plate1	29	D	2	1843092	d4
GF-d4-Plate1-25183-30	25183	GF	Plate1	30	E	1	3678838	d4
GF-d4-Plate2-25208-35	25208	GF	Plate2	35	D	9	3470625	d4
WJL-d4-Plate1-25210-38	25210	WJL	Plate1	38	D	6	3828526	d4
GF-d4-Plate1-25210-39	25210	GF	Plate1	39	E	5	4247231	d4
GF-d4-Plate2-25183-41	25183	GF	Plate2	41	F	1	1761823	d4
GF-d4-Plate2-25210-43	25210	GF	Plate2	43	F	5	3169382	d4
WJL-d4-Plate1-25208-46	25208	WJL	Plate1	46	C	10	2892171	d4
WJL-d4-Plate1-25208-47	25208	WJL	Plate1	47	B	10	3387926	d4
WJL-d4-Plate1-25183-48	25183	WJL	Plate1	48	F	2	3595814	d4
WJL-d4-Plate1-25208-50	25208	WJL	Plate1	50	A	10	5708076	d4
WJL-d4-Plate1-25208-52	25208	WJL	Plate1	52	E	10	3305828	d4
WJL-d4-Plate1-25208-54	25208	WJL	Plate1	54	D	10	2980174	d4
WJL-d4-Plate1-25208-55	25208	WJL	Plate1	55	F	10	2648893	d4
GF-d4-Plate2-25208-57	25208	GF	Plate2	57	F	9	1789505	d4
GF-d4-Plate1-25183-59	25183	GF	Plate1	59	F	1	3461758	d4
GF-d4-Plate1-25210-60	25210	GF	Plate1	60	F	5	3205718	d4
WJL-d4-Plate2-25183-64	25183	WJL	Plate2	64	F	2	3165014	d4
GF-d4-Plate1-25208-67	25208	GF	Plate1	67	F	9	1551867	d4
WJL-d4-Plate2-25210-70	25210	WJL	Plate2	70	F	6	8073425	d4
GF-d4-Plate1-25208-72	25208	GF	Plate1	72	C	9	2668655	d4
GF-d4-Plate2-25210-74	25210	GF	Plate2	74	B	5	947737	d4
WJL-d4-Plate2-25210-75	25210	WJL	Plate2	75	C	6	4812520	d4
GF-d4-Plate2-25183-78	25183	GF	Plate2	78	B	1	2869820	d4
WJL-d4-Plate2-25183-79	25183	WJL	Plate2	79	C	2	4934533	d4
GF-d4-Plate1-25210-83	25210	GF	Plate1	83	C	5	4113175	d4
WJL-d4-Plate1-25210-84	25210	WJL	Plate1	84	B	6	4684552	d4
GF-d4-Plate2-25208-86	25208	GF	Plate2	86	B	9	3324070	d4
GF-d4-Plate1-25183-87	25183	GF	Plate1	87	C	1	3728767	d4
WJL-d4-Plate1-25183-88	25183	WJL	Plate1	88	B	2	4564509	d4
WJL-d4-Plate1-25210-90	25210	WJL	Plate1	90	C	6	3714293	d4
GF-d4-Plate1-25210-91	25210	GF	Plate1	91	B	5	4179985	d4
GF-d4-Plate2-25208-93	25208	GF	Plate2	93	C	9	3569201	d4
WJL-d4-Plate1-25183-94	25183	WJL	Plate1	94	C	2	4200621	d4
GF-d4-Plate1-25183-95	25183	GF	Plate1	95	B	1	4373035	d4
GF-d4-Plate1-25208-98	25208	GF	Plate1	98	B	9	3652231	d4
WJL-d4-Plate2-25210-101	25210	WJL	Plate2	101	B	6	4457721	d4
GF-d4-Plate2-25210-103	25210	GF	Plate2	103	C	5	3903565	d4
WJL-d4-Plate2-25183-104	25183	WJL	Plate2	104	B	2	982388	d4
GF-d4-Plate2-25183-105	25183	GF	Plate2	105	C	1	3094592	d4
GF-d4-Plate2-25208-110	25208	GF	Plate2	110	A	9	1967561	d4
WJL-d4-Plate1-25210-112	25210	WJL	Plate1	112	A	6	3472086	d4

WJL-d4-Plate1-25183-116	25183	WJL	Plate1	116	A	2	4865847	d4
GF-d4-Plate2-25210-119	25210	GF	Plate2	119	A	5	3773438	d4
WJL-d4-Plate2-25208-120	25208	WJL	Plate2	120	F	10	2018688	d4
WJL-d4-Plate2-25208-121	25208	WJL	Plate2	121	D	10	2595705	d4
WJL-d4-Plate2-25208-123	25208	WJL	Plate2	123	E	10	1841390	d4
WJL-d4-Plate2-25208-124	25208	WJL	Plate2	124	A	10	3326544	d4
GF-d4-Plate2-25183-125	25183	GF	Plate2	125	A	1	1822797	d4
WJL-d4-Plate2-25208-126	25208	WJL	Plate2	126	B	10	3831425	d4
WJL-d4-Plate2-25208-127	25208	WJL	Plate2	127	C	10	3109485	d4
WJL-d4-Plate2-25210-129	25210	WJL	Plate2	129	A	6	1737064	d4
GF-d4-Plate1-25208-132	25208	GF	Plate1	132	A	9	3284211	d4
WJL-d4-Plate2-25183-135	25183	WJL	Plate2	135	A	2	4603643	d4
GF-d4-Plate1-25210-139	25210	GF	Plate1	139	A	5	2749602	d4
GF-d4-Plate1-25183-140	25183	GF	Plate1	140	A	1	2722703	d4

750 **Reference**

- 751 1. Flatt, T. (2005). The evolutionary genetics of canalization. *Q Rev Biol* *80*, 287-316.
- 752 2. Rutherford, S., Hirate, Y., and Swalla, B.J. (2007). The Hsp90 capacitor, developmental
753 remodeling, and evolution: the robustness of gene networks and the curious evolvability
754 of metamorphosis. *Crit Rev Biochem Mol Biol* *42*, 355-372.
- 755 3. Wagner, A. (2007). Robustness and Evolvability in Living Systems. , Paperback Edition,
756 (Princeton University Press).
- 757 4. Brucker, R.M., and Bordenstein, S.R. (2013). The hologenomic basis of speciation: gut
758 bacteria cause hybrid lethality in the genus *Nasonia*. *Science* *341*, 667-669.
- 759 5. Rosenberg, E., and Zilber-Rosenberg, I. (2011). Symbiosis and development: the
760 hologenome concept. *Birth Defects Res C Embryo Today* *93*, 56-66.
- 761 6. Douglas, A.E. (2014). Symbiosis as a general principle in eukaryotic evolution. *Cold
762 Spring Harb Perspect Biol* *6*.
- 763 7. Storelli, G., Strigini, M., Grenier, T., Bozonnet, L., Schwarzer, M., Daniel, C., Matos, R.,
764 and Leulier, F. (2017). Drosophila Perpetuates Nutritional Mutualism by Promoting the
765 Fitness of Its Intestinal Symbiont *Lactobacillus plantarum*. *Cell metabolism*.
- 766 8. Storelli, G., Defaye, A., Erkosar, B., Hols, P., Royet, J., and Leulier, F. (2011).
767 *Lactobacillus plantarum* promotes *Drosophila* systemic growth by modulating hormonal
768 signals through TOR-dependent nutrient sensing. *Cell metabolism* *14*, 403-414.
- 769 9. Erkosar, B., Storelli, G., Mitchell, M., Bozonnet, N., Leulier, F. (2015). Pathogen
770 virulence impedes mutualist-mediated enhancement of host protein digestion capacity
771 and juvenile growth. *in review*.
- 772 10. Lehner, B. (2013). Genotype to phenotype: lessons from model organisms for human
773 genetics. *Nature reviews. Genetics* *14*, 168-178.
- 774 11. Alpern, D., Gardeux, V., Russeil, J., and Deplancke, B. (2018). Time- and cost-efficient
775 high-throughput transcriptomics enabled by Bulk RNA Barcoding and sequencing.
776 *bioRxiv*.
- 777 12. Erkosar, B., Defaye, A., Bozonnet, N., Puthier, D., Royet, J., and Leulier, F. (2014).
778 *Drosophila* microbiota modulates host metabolic gene expression via IMD/NF- κ B
779 signaling. *PloS one* *9*, e94729.
- 780 13. Mestek Boukhibar, L., and Barkoulas, M. (2016). The developmental genetics of
781 biological robustness. *Annals of botany* *117*, 699-707.
- 782 14. Posadas, D.M., and Carthew, R.W. (2014). MicroRNAs and their roles in developmental
783 canalization. *Current opinion in genetics & development* *27*, 1-6.
- 784 15. Tefit, M.A., Gillet, B., Joncour, P., Hughes, S., and Leulier, F. (2017). Stable association
785 of a *Drosophila*-derived microbiota with its animal partner and the nutritional
786 environment throughout a fly population's life cycle. *J Insect Physiol*.
- 787 16. Rohner, N., Jarosz, D.F., Kowalko, J.E., Yoshizawa, M., Jeffery, W.R., Borowsky, R.L.,
788 Lindquist, S., and Tabin, C.J. (2013). Cryptic variation in morphological evolution:
789 HSP90 as a capacitor for loss of eyes in cavefish. *Science* *342*, 1372-1375.
- 790 17. Rutherford, S.L., and Lindquist, S. (1998). Hsp90 as a capacitor for morphological
791 evolution. *Nature* *396*, 336-342.
- 792 18. Queitsch, C., Sangster, T.A., and Lindquist, S. (2002). Hsp90 as a capacitor of
793 phenotypic variation. *Nature* *417*, 618-624.
- 794 19. Mirth, C.K., and Shingleton, A.W. (2012). Integrating body and organ size in *Drosophila*:
795 recent advances and outstanding problems. *Frontiers in endocrinology* *3*, 49.
- 796 20. Waddington, C.H. (1959). Canalization of development and genetic assimilation of
797 acquired characters. *Nature* *183*, 1654-1655.
- 798 21. Santabarbara-Ruiz, P., Lopez-Santillan, M., Martinez-Rodriguez, I., Binagui-Casas, A.,
799 Perez, L., Milan, M., Corominas, M., and Serras, F. (2015). ROS-Induced JNK and p38
800 Signaling Is Required for Unpaired Cytokine Activation during *Drosophila* Regeneration.
801 *PLoS genetics* *11*, e1005595.
- 802 22. Jones, R.M., Luo, L., Arditia, C.S., Richardson, A.N., Kwon, Y.M., Mercante, J.W.,
803 Alam, A., Gates, C.L., Wu, H., Swanson, P.A., et al. (2013). Symbiotic *lactobacilli*

804 stimulate gut epithelial proliferation via Nox-mediated generation of reactive oxygen
805 species. *EMBO J* 32, 3017-3028.

806 23. Jones, R.M., Desai, C., Darby, T.M., Luo, L., Wolfarth, A.A., Scharer, C.D., Ardita, C.S.,
807 Reedy, A.R., Keebaugh, E.S., and Neish, A.S. (2015). Lactobacilli Modulate Epithelial
808 Cytoprotection through the Nrf2 Pathway. *Cell Rep* 12, 1217-1225.

809 24. Broderick, N.A., Buchon, N., and Lemaitre, B. (2014). Microbiota-induced changes in
810 *drosophila melanogaster* host gene expression and gut morphology. *mBio* 5, e01117-
811 01114.

812 25. Wong, A.C., Chaston, J.M., and Douglas, A.E. (2013). The inconstant gut microbiota of
813 *Drosophila* species revealed by 16S rRNA gene analysis. *The ISME journal* 7, 1922-
814 1932.

815 26. Elgart, M., Stern, S., Salton, O., Gnainsky, Y., Heifetz, Y., and Soen, Y. (2016). Impact
816 of gut microbiota on the fly's germ line. *Nature communications* 7, 11280.

817 27. Bates, D., Mächler M, Bolker B, Walker S (2015). Fitting Linear Mixed-Effects Models
818 Using lme4. *Journal of Statistical Software* 67, 1-48.

819 28. Huang, W., Massouras, A., Inoue, Y., Peiffer, J., Ramia, M., Tarone, A.M., Turlapati, L.,
820 Zichner, T., Zhu, D., Lyman, R.F., et al. (2014). Natural variation in genome architecture
821 among 205 *Drosophila melanogaster* Genetic Reference Panel lines. *Genome research* 24,
822 1193-1208.

823 29. Mackay, T.F., Richards, S., Stone, E.A., Barbadilla, A., Ayroles, J.F., Zhu, D., Casillas,
824 S., Han, Y., Magwire, M.M., Cridland, J.M., et al. (2012). The *Drosophila melanogaster*
825 Genetic Reference Panel. *Nature* 482, 173-178.

826 30. Dobin, A., Davis, C.A., Schlesinger, F., Drenkow, J., Zaleski, C., Jha, S., Batut, P.,
827 Chaisson, M., and Gingeras, T.R. (2013). STAR: ultrafast universal RNA-seq aligner.
828 *Bioinformatics* 29, 15-21.

829 31. Law, C.W., Chen, Y., Shi, W., and Smyth, G.K. (2014). voom: Precision weights unlock
830 linear model analysis tools for RNA-seq read counts. *Genome biology* 15, R29.

831 32. Ritchie, M.E., Phipson, B., Wu, D., Hu, Y., Law, C.W., Shi, W., and Smyth, G.K. (2015).
832 limma powers differential expression analyses for RNA-sequencing and microarray
833 studies. *Nucleic acids research* 43, e47.

834 33. Schneider, C.A., Rasband, W.S., and Eliceiri, K.W. (2012). NIH Image to ImageJ: 25
835 years of image analysis. *Nature methods* 9, 671-675.

836 34. Ryu, J.H., Kim, S.H., Lee, H.Y., Bai, J.Y., Nam, Y.D., Bae, J.W., Lee, D.G., Shin, S.C.,
837 Ha, E.M., and Lee, W.J. (2008). Innate immune homeostasis by the homeobox gene
838 caudal and commensal-gut mutualism in *Drosophila*. *Science* 319, 777-782.

839 35. Hu, Y., Comjean, A., Perkins, L.A., Perrimon, N., and Mohr, S.E. (2015). GLAD: an
840 Online Database of Gene List Annotation for *Drosophila*. *J Genomics* 3, 75-81.

841 36. Powell, J.A. (2014). GO2MSIG, an automated GO based multi-species gene set generator
842 for gene set enrichment analysis. *BMC Bioinformatics* 15, 146.

843 37. Saunders, A., Werner, J., Andrulis, E.D., Nakayama, T., Hirose, S., Reinberg, D., and
844 Lis, J.T. (2003). Tracking FACT and the RNA polymerase II elongation complex through
845 chromatin in vivo. *Science* 301, 1094-1096.

846 38. Shimojima, T., Okada, M., Nakayama, T., Ueda, H., Okawa, K., Iwamatsu, A., Handa,
847 H., and Hirose, S. (2003). *Drosophila* FACT contributes to Hox gene expression through
848 physical and functional interactions with GAGA factor. *Genes & development* 17, 1605-
849 1616.

850

851